informa
healthcare

Inhibition of choline oxidase by quinoid dyes

ÖZDEN TACAL & INCI ÖZER

Department of Biochemistry, School of Pharmacy, Hacettepe University, 06100 Ankara, Turkey

Abstract
Choline oxidase catalyzes the oxidation of choline to glycine-betaine, with betaine-aldehyde as intermediate and molecular oxygen as primary electron acceptor. This study reports on the inhibitory effects of triarylmethanes (*cationic* malachite green; *neutral* leukomalachite green), phenoxazines (*cationic*, meldola blue and nile blue; *neutral* nile red) and a structurally-related phenothiazine (methylene blue) on choline oxidase, assayed at 25°C in 50 mM MOPS buffer, pH 7, using choline as substrate. Methylene B acted as a competitive inhibitor with $K_i = 74 \pm 7.2\,\mu M$, pointing to the choline–binding site of the enzyme as a target site. Nile B caused noncompetitive inhibition of enzyme activity with $K_i = 20 \pm 4.5\,\mu M$. In contrast to methylene B and nile B, malachite G and meldola B caused complex, nonlinear inhibition of choline oxidase, with estimated K_i values in the micromolar range. The difference in kinetic pattern was ascribed to the differential ability of the dyes to interact (and interfere) with the flavin cofactor, generating different perturbations in the steady-state balance of the catalytic process.

Keywords: *Choline oxidase, enzyme inhibition, malachite green, meldola blue, nile blue, methylene blue*

Abbreviations: *CHO, choline oxidase; HRP, horseradish peroxidase; leucomalachite G, leucomalachite green; malachite G, malachite green; meldola B, meldola blue; methylene B, methylene blue; MOPS, 3-(N-morpholino)propanesulfonic acid; nile B, nile blue; nile R, nile red*

Introduction

Choline oxidase (CHO, E.C. 1.1.3.17) is a FAD-containing enzyme that catalyzes the oxidation of choline to glycine-betaine, with betaine-aldehyde as intermediate and molecular oxygen as primary electron acceptor (Scheme I). Being one of the few flavoproteins that carry out a four-electron oxidation of an alcohol to a carboxylic acid through an aldehyde intermediate, the enzyme has been subjected to detailed mechanistic studies [1,2]. In addition, the need to develop biosensors for the detection of choline and choline esters such as acetylcholine in serological samples and foods has focused clinical and industrial interest on the enzyme as an analytical tool [3,4]. Since many bacterial and plant species accumulate glycine-betaine in response to various conditions such as osmotic stress and extreme temperatures, CHO promises to be of further value in relation to the development of therapeutic agents and the design of genetically modified, drought-resistant crop plants [5–7].

CHO has been purified and characterized from *Arthrobacter globiformis* [8] and *Alcaligenes sp.* [9] and the fungus, *Cylindrocarbon didymium* [10]. The choline oxidase gene of *A. globiformis* has recently been cloned and sequenced [11]. The resulting protein is a homodimer of 120 kDa, with each subunit containing covalently bound FAD in 8α-N(1)-histidyl linkage [12,13]. The catalytic mechanism of the enzyme has been elucidated by using kinetic and spectroscopic methods [14–18].

Relatively little is known about the active site topology and the substrate and inhibitor specificity of CHO. The trimethylammonium group is a major structural determinant for substrate turnover. Competitive inhibition studies point to the involvement of alkyl-substituted amine headgroups in inhibitor binding ($K_i = 2–26\,mM$) [19]. In the present study, aiming to identify further structural preferences in

Correspondence: Ö. Tacal, Fax:(90) 312-3114777. E-mail: tacal@hacettepe.edu.tr
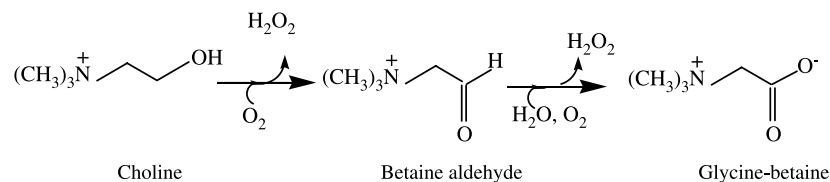
Scheme 1.   Oxidation of choline by choline oxidase.

ligand binding, we have tested the effects of a selection of dyes/leukodyes on choline oxidase activity. The selection includes triarylmethanes (*cationic* malachite green; *neutral* leukomalachite green), phenoxazines (*cationic*, meldola blue and nile blue; *neutral* nile red) and a structurally-related phenothiazine (methylene blue) (Figure 1). Earlier work in our laboratory has shown that malachite G, meldola B and nile B can reversibly bind to (or form adducts with) a variety of proteins and protein-related nucleophiles [20–22]. More specifically, they are highly effective as inhibitors of plasma cholinesterase, with K_i values in the μM range [23]. The phenothiazine ring system is a structural feature of a series of cholinesterase inhibitors which have been studied in detail [24,25]. The cationic dyes were therefore tested for their potential to inhibit choline oxidase as well. The neutral species (leucomalachite G and nile R) were included in the study for comparative purposes. The preliminary results reported here show that the charged dyes bind CHO with 2–3 orders of magnitude higher affinity than the choline analogues

cited in reference [19] and might be helpful in the design of new CHO inhibitors.

Materials and methods

Horseradish peroxidase (HRP, E.C. 1.11.1.7, Type VI A), choline oxidase (E.C. 1.1.3.17, from *Alcaligenes sp.*), malachite G hydrochloride, leucoma-lachite G, meldola B, methylene B, nile B chloride and nile R were purchased from Sigma-Aldrich (USA). All remaining chemicals were obtained from Sigma-Aldrich or Merck (Germany). Stock solutions of the ligands (5 mM) were prepared in dimethyl sulfoxide.

Measurement of choline oxidase activity

Choline oxidase activity was assayed spectrophoto-metrically at 25°C, in the presence of HRP and *o*-dianisidine as the chromogenic component. The assay mixture (1.2 ml) contained 50 mM MOPS buffer (pH 7), 0.1–0.4 mM choline as substrate,
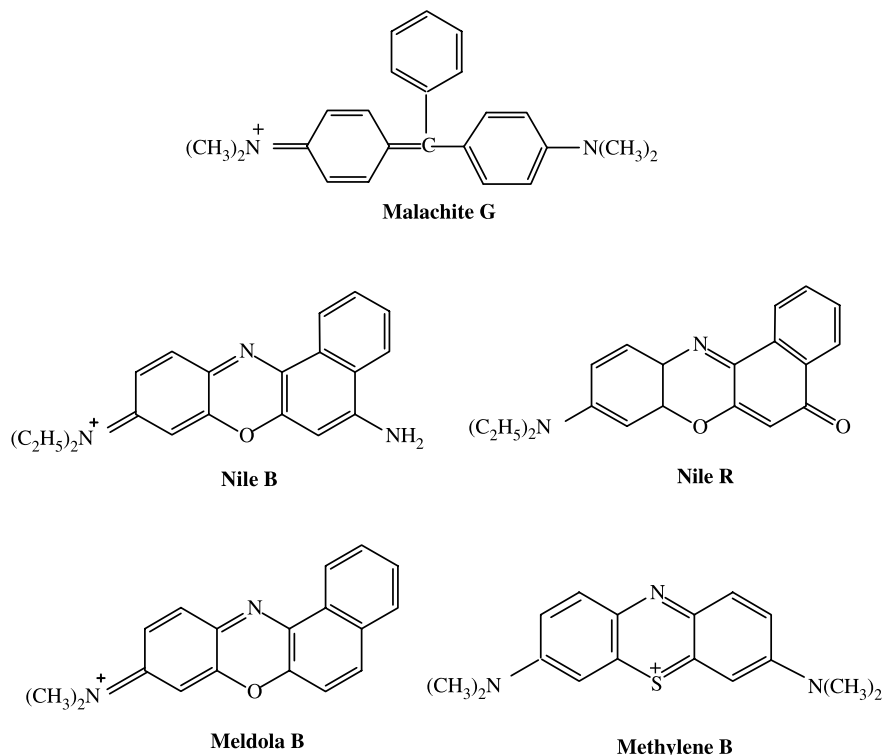

Figure 1.   The quinoid dyes studied.

4.2 U HRP, 0.16 mM *o*-dianisidine. The reactions were initiated by adding ca. 0.3 U/ml CHO (20 µl), followed by 0–40 µM dye ($\leq$ 20 µl). The progress of the *o*-dianisidine oxidation was monitored by the increase in absorbance at 500 nm, using a Shimadzu 1601 PC spectrophotometer equipped with a Peltier unit. CHO activity was calculated using the linear segments of the progress curves in the initial 60-s period (ε_{500}, *o*-dianisidine $= 13.5 \text{ mM}^{-1} \text{ cm}^{-1}$, determined in this study).

The potential of the dyes to affect HRP activity was tested by assaying the indicator enzyme in the presence and absence of 40 µM dye. The assays were carried out at 25°C, in 50 mM MOPS buffer (pH 7) containing 0.16 mM *o*-dianisidine, 2 mM H_2O_2. The reactions were started by the addition of HRP (3 mU/ml) and the oxidation of *o*-dianisidine was monitored as above. HRP activity was found to be inhibited by < 20%, i.e. not to an extent which would render the chromogenic system rate-limiting in the CHO assay. The stability of the dyes in the assay system was verified spectroscopically. No redox changes were detected.

Results and discussion

All ligands tested were found to act as reversible, linear inhibitors of choline oxidase. The initial rate data were analyzed using a simplified rapid equilibrium model for linear inhibition (Scheme II) and the corresponding rate equations (Equations 1 and 2) [26].
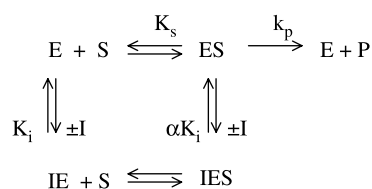
$$v = \frac{V_{max}[S]_o}{K_s(1 + [I]/K_i) + [S]_o(1 + [I]/\alpha K_i)} \quad (1)$$

$$v^{-1} = \frac{[S]_o + \alpha K_s}{\alpha K_i V_{max}[S]_o}[I] + \frac{[S]_o + K_s}{V_{max}[S]_o}$$
$$\text{(Dixon Equation)} \quad (2)$$

Relative inhibitory potencies

Inhibitory potencies were compared on the basis of intercept/slope (i.e. apparent K_i or I_{50}) values derived from Dixon plots of v^{-1} *versus* [I] at 0.1 mM choline. The results are given in Table I. All 6 ligands were effective as choline oxidase inhibitors; the I_{50} values

Scheme 2. Rapid equilibrium model for linear inhibition.

Table I. Choline oxidase inhibitory potencies of triarylmethane, phenoxazine and phenothiazine dyes.

Compound	I_{50}, µM[a,b]
Nile blue	18 ± 2.8
Meldola blue	24 ± 4.3
Methylene blue	89 ± 3.8
Malachite green	29 ± 8.7
Nile red	120 ± 3.1
Leukomalachite green	140 ± 6.2

[a][choline]$_o$ = 0.1 mM; [b]Selected K_i values (mM) for choline analogs [19]: trimethylamine, 2.4; diethylmethylamine, 5; trimethylethylamine, 13; allyltrimethylamine, 15.

for the cationic species were 100- to 800-fold lower than the K_i values of the aliphatic choline analogues previously studied [19]. The 3- to 6-fold difference between the affinities of the charged and neutral or leuko ligands is similar to the differential affinity of CHO for its substrates, choline ($K_m = 0.43$ mM) and 3,3-dimethyl-1-butanol ($K_m = 1$ mM) [19], suggesting that charge-charge interactions are not primary determinants in ligand selectivity and pointing to a major hydrophobic driving force in enzyme-inhibitor complex formation.

Notes on the inhibitory mechanism

The effects of the cationic dyes were analyzed in greater detail at multiple $[S]_o$ and [I] values. The resultant family of Dixon plots was utilized to construct diagnostic slope replots according to Equation (3): Scheme II requires

$$\text{Slope, Eq. 2} = \frac{K_s}{K_i V_{max}[S]_o} + \frac{1}{\alpha K_i V_{max}} \quad (3)$$

that the slope replot intersect the abscissa at [I] = 0, $-1/K_s$ or $-1/\alpha K_s$, depending on whether the inhibitor has a competitive, noncompetitive or mixed effect on substrate binding and turnover [26].

Dixon plots and the slope replot of the inhibition of CHO by methylene B are given in Figure 2. The slope replot (Figure 2B) for the phenothiazine dye pointed to a competitive pattern of inhibition ($\alpha = \infty$), with $K_i = 74 \pm 7.2$ µM (based on Equation (3) and $K_s/V_{max} = 32.3 \pm 2.84$ min as determined in independent experiments). The corresponding slope replot of the inhibition by nile B (Figure 3a) indicated noncompetitive inhibition with $K_i = 20 \pm 4.5$ µM. In contrast to methylene B and nile B, the slope replots for inhibition by meldola B and malachite G were inconsistent with Scheme II operating under rapid equilibrium conditions. The plot for meldola B (Figure 3b), while seemingly linear ($r^2 = 0.985$), yielded a positive abscissa intercept if processed as a straight line (i.e. a negative value for K_s or α). The inconsistency was even more pronounced in the case
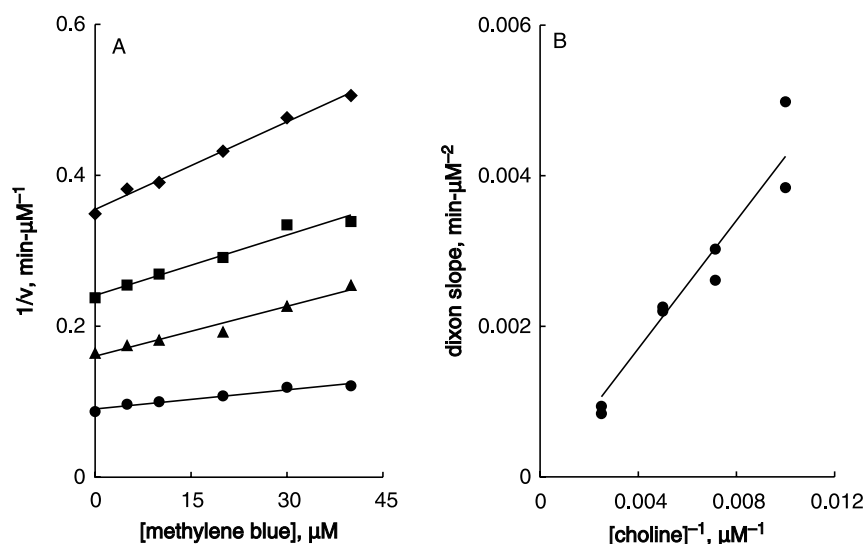
Figure 2.   The inhibition of choline oxidase by methylene blue. A. Dixon plots of inhibition at 0.1 (◆), 0.14 (■), 0.2 (▲) and 0.4 (●) mM choline. (Average of 2 independent experiments). B. Slope replot (showing independent data sets).

of malachite G, where the slope replots showed pronounced curvature (Figure 3c).

The irregularity of the inhibition data for meldola B and malachite G was taken to reflect the complex nature of the multi-step, steady-state CHO system: In steady-state systems, the initial rate equation for competitive inhibition ($\alpha = \infty$) has the same form as the corresponding equation for a rapid equilibrium scheme. Steady-state initial rate equations for non-competitive and linear mixed inhibition ($1 \leq \alpha < \infty$), on the other hand, contain second-order terms in [S] and [I] [27]. Thus plots based on Equations (2) and (3) are both potentially nonlinear. In the present case, $[S]^2$ was apparently the only higher-order term to make a significant contribution within the experimental ranges of [I] and [S], such that only the slope replots deviated from linearity. Proceeding with the assumption of steady-state, noncompetitive (or linear mixed) inhibition, the replots for meldola B and malachite G were fitted to an exponential trendline and αK_i was estimated from the ordinate intercepts with reference to Equation (3) ($V_{max}^{-1} = 0.036 \pm 0.003$ min $- \mu M^{-1}$). The αK_i estimates for meldola B and malachite G were 33 ± 6.5 and $34 \pm 3.3 \mu M$, respectively, and in reasonable agreement with the I_{50} values in Table I.

In conclusion, the results of this study show that choline oxidase can bind and is susceptible to inhibition by a variety of molecules with quinoid structural elements. The competitive nature of the inhibition by methylene B points to the choline-binding site of the enzyme as a target site. The inhibition by nile B, meldola B and malachite G is noncompetitive with respect to choline (but
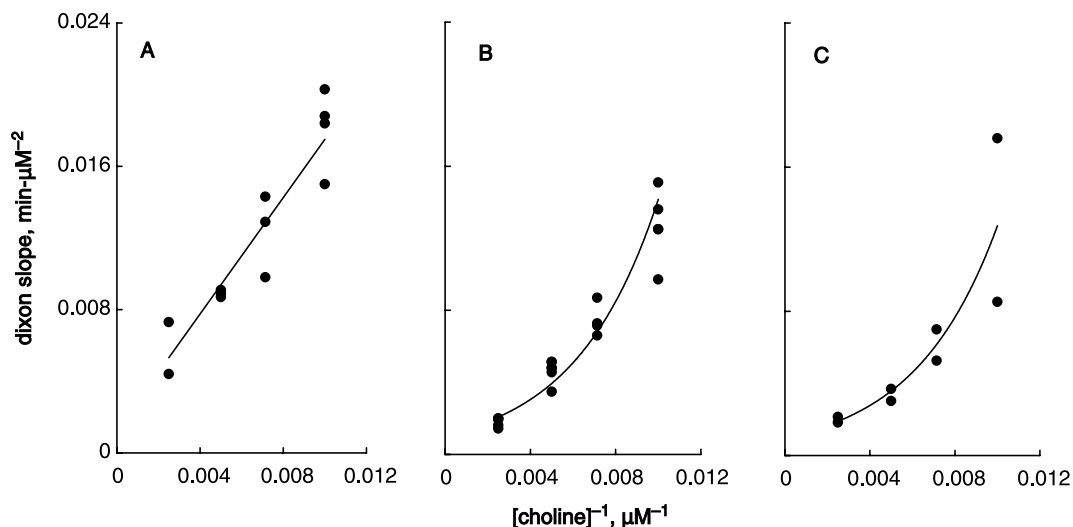

Figure 3.   Slope replots of the inhibition of choline oxidase by nile blue (A), meldola blue (B) and malachite green (C).

might further have a competitive component obscured by the complexity of the inhibition patterns). The predominantly noncompetitive nature of inhibition by these dyes implicates the flavin-binding site as a possible target. Why structurally similar species such as methylene blue, nile B, meldola B and malachite G exert distinct effects on choline oxidase is not immediately obvious. The difference may stem from the differential ability of the dyes to interact (and interfere) with the flavin cofactor, generating different perturbations in the steady-state balance of the catalytic process. A study on the impact of binding on the spectral properties of the dye and flavin moieties should provide information regarding the proximity of the inhibitor binding domain to the redox active site of the enzyme.

Acknowledgements

References

[1] Gadda G. Kinetic mechanism of choline oxidase from arthrobacter globiformis. Biochim Biophys Acta 2003;1646: 112–118.

[2] Fan F, Germann MW, Gadda G. Mechanistic studies of choline oxidase with betaine aldehyde and its isosteric analogue 3,3-dimethylbutyraldehyde. Biochemistry 2006;45: 1979–1986.

[3] Kok FN, Bozoglu F, Hasirci V. Construction of an acetylcholinesterase-choline oxidase biosensor for aldicarb determination. Biosens Bioelectron 2002;17:531–539.

[4] Razola SS, Pochet S, Grosfils K, Kauffmann JM. Ampero-metric determination of choline released from rat submandi-bular gland acinar cells using a choline oxidase biosensor. Biosens Bioelectron 2003;18:185–191.

[5] Sakamoto A, Murata N. The use of bacterial choline oxidase, a glycinebetaine-synthesizing enzyme, to create stress-resistant transgenic plants. Plant Physiol 2001;125:180–188.

[6] Huang J, Hirji R, Adam L, Rozwadowski KL, Hammerlindl JK, Keller WA, Selvaraj G. Genetic engineering of glycinebetaine production toward enhancing stress tolerance in plants: Metabolic limitations. Plant Physiol 2000;122:747–756.

[7] Rozwadowski KL, Khachatourians GG, Selvaraj G. Choline oxidase, a catabolic enzyme in arthrobacter pascens, facilitates adaptation to osmotic stress in escherichia coli. J Bacteriol 1991;173:472–478.

[8] Ikuta S, Imamura S, Misaki H, Horiuti Y. Purification and characterization of choline oxidase from arthrobacter globi-formis. J Biochem (Tokyo) 1977;82:1741–1749.

[9] Ohta-Fukuyama M, Miyake Y, Emi S, Yamano T. Identi-fication and properties of the prosthetic group of choline oxidase from alcaligenes sp. J Biochem (Tokyo) 1980;88: 197–203.

[10] Lartillot S. A simplified method of production of choline oxidase suitable for choline assay. Prep Biochem 1987;17: 283–295.

[11] Fan F, Ghanem M, Gadda G. Cloning, sequence analysis and purification of choline oxidase from arthrobacter globiformis: A bacterial enzyme involved in osmotic stress tolerance. Arch Biochem Biophys 2004;421:149–158.

[12] Ghanem M, Fan F, Francis K, Gadda G. Spectroscopic and kinetic properties of recombinant choline oxidase from arthrobacter globiformis. Biochemistry 2003;42:15179–15188.

[13] Rand T, Halkier T, Hansen OC. Structural characterization and mapping of the covalently linked FAD cofactor in choline oxidase from arthrobacter globiformis. Biochemistry 2003;42:7188–7194.

[14] Fan F, Gadda G. On the catalytic mechanism of choline oxidase. J Am Chem Soc 2005;127:2067–2074.

[15] Ghanem M, Gadda G. On the catalytic role of the conserved active site residue His466 of choline oxidase. Biochemistry 2005;44:893–904.

[16] Fan F, Gadda G. Oxygen- and temperature-dependent kinetic isotope effects in choline oxidase: Correlating reversible hydride transfer with environmentally enhanced tunneling. J Am Chem Soc 2005;127:17954–17961.

[17] Gadda G. pH and deuterium kinetic isotope effects studies on the oxidation of choline to betaine-aldehyde catalyzed by choline oxidase. Biochim Biophys Acta 2003;1650:4–9.

[18] Ghanem M, Gadda G. Effects of reversing the protein positive charge in the proximity of the flavin n(1) locus of choline oxidase. Biochemistry 2006;45:3437–3447.

[19] Gadda G, Powell NL, Menon P. The trimethylammonium head group of choline is a major determinant for substrate binding and specificity in choline oxidase. Arch Biochem Biophys 2004;430:264–273.

[20] Eldem Y, Ozer I. Electrophilic reactivity of cationic triarylmethane dyes towards proteins and protein-related nucleophiles. Dyes Pigments 2004;60:49–54.

[21] Tacal O, Ozer I. Adduct-forming tendencies of cationic triarylmethane dyes with proteins: Metabolic and toxicological implications. J Biochem Mol Toxicol 2004;18:253–256.

[22] Ozer I. Reactivity of meldola blue towards sulfhydryl groups: Analytical and biomedical aspects. Turk J Biochem 2005;30:220–224.

[23] Kucukkilinc T, Ozer I. Inhibition of human plasma cholinesterase by malachite green and related triarylmethane dyes: Mechanistic implications. Arch Biochem Biophys 2005;440:118–122.

[24] Saxena A, Fedorko JM, Vinayaka CR, Medhekar R, Radic Z, Taylor P, Lockridge O, Doctor BP. Aromatic amino-acid residues at the active and peripheral anionic sites control the binding of E2020 (Aricept) to cholinesterases. Eur J Biochem 2003;270:4447–4458.

[25] Radic Z, Pickering NA, Vellom DC, Camp S, Taylor P. Three distinct domains in the cholinesterase molecule confer selectivity for acetyl- and butyrylcholinesterase inhibitors. Biochemistry 1993;32:12074–12084.

[26] Segel IH. Enzyme Kinetics, New York: Wiley-Interscience; 1975. p 170–176.

[27] Segel IH. Enzyme Kinetics, New York: Wiley-Interscience; 1975. p 199–202.